

**Zero-flow: A novel approach to continuous ultrasonic welding of
CF/PPS thermoplastic composite plates**

Frank Senders, Martijn van Beurden, Genevieve Palardy, Irene F. Villegas*

Aerospace Structures and Materials Department, Delft University of Technology,

Kluyverweg 1, 2629 HS Delft, The Netherlands

senders.frank@gmail.com, mvanb1@gmail.com, g.palardy@tudelft.nl (+31 15 27
83626, orcid.org/0000-0003-3142-8782) and I.FernandezVillegas@tudelft.nl* (+31 15
27 89745, orcid.org/0000-0003-3740-0123)

Zero-flow: A novel approach to continuous ultrasonic welding of CF/PPS thermoplastic composite plates

Continuous ultrasonic welding of plastic films, fabrics and even thermoplastic composite prepreg tape is common industrial practice. However, continuous ultrasonic welding of stiff thermoplastic composite plates is challenging due to squeeze flow of resin at the welding interface, and significant local deformation of the welding stack, that are generally needed to achieve strong welds. This paper presents a novel approach to continuous ultrasonic welding of thermoplastic composite plates based on zero-flow welding. The proposed technique can create strong welds before any squeeze flow takes place at the interface. It is enabled by the use of very thin flat energy directors, owing to simultaneous melting of both energy director and adherends' matrix. The results prove the feasibility and indicate the potential for high-strength welds between thermoplastic composite plates at very high speed.

Keywords: Composites; Thermoplastic resin; Structural joining; Fusion bonding; Ultrasonic heating; Continuous welding

Introduction

Ultrasonic welding is a very promising technique for assembling thermoplastic composite (TPC) structures. It features extremely short heating times and very low energy consumption [1]. Ultrasonic heat generation is mostly restricted to the welding interface and hence, the process results in very narrow heat affected zones [2]. Energy directors (EDs), which in the case of unreinforced plastics are most commonly triangular resin protrusions moulded on the welding surfaces [3], are used to concentrate heat generation at the interface. These traditional triangular energy directors have also been used for ultrasonic welding of thermoplastic composites. However the so-called “flat energy directors”, i.e. thin films of neat resin placed at the welding interface prior

to the welding process, have been proven as a successful and straightforward alternative for the welding of thermoplastic composites [4]. Ultrasonic welding is a versatile process, and unlike resistance and induction welding, can be applied independently from the type of fiber reinforcement in the composite parts to be welded [1]. Moreover, it offers the possibility of in-situ process monitoring [5,6], which allows for efficient definition of optimum process parameters [7], or to implement closed-loop welding or in-situ quality assessment.

One of the major shortcomings of ultrasonic welding of thermoplastic composites is that it is known as a spot welding technique. However, in most structural applications, continuously welded seams are preferred. As a result, other techniques that allow a more straightforward implementation of continuous welding processes for thermoplastic composites have drawn further attention from researchers and industry in the last years [8,9,10]. Today, very little information can be found in the literature on the production of continuous ultrasonically welded seams in thermoplastic composite plates or parts. Lu et al. discussed a sequential ultrasonic process for carbon fibre (CF)/polyetheretherketone (PEEK) to continuously join 635 mm-long seams using multiple coalescent welded spots [11]. They used energy director films with moulded triangles in between the adherends and mentioned successful results. Soccad filed a patent application in 2007 on an ultrasonic assembly method [12] according to which the sonotrode continuously moves on top of the intended welding overlap while a compressive force is applied on the opposite side. In this method, one or both of the adherends are provided with protruding energy directors on their welding surfaces. Levy et al. have used a continuous welding apparatus to qualitatively validate some of their numerical results concerning flow of triangular energy directors [13]. However, no

further results concerning the continuous ultrasonic welding process described in [12] can be found in the open literature.

Based on the work presented by Palardy et al. [14], one of the main challenges to implement continuous ultrasonic welding of thermoplastic composite parts is the squeeze flow of the energy director. As widely acknowledged, the development of satisfactory weld strength during a regular static ultrasonic welding process is accompanied by squeeze flow of the molten energy director and hence, downward displacement of the sonotrode [5-7,13]. This squeeze flow was found to be necessary for both triangular [5,13,15] and flat energy directors [6,7]. Local squeeze flow during a continuous ultrasonic welding process requires at least one of the adherends be flexible enough to accommodate temporarily non-uniform thicknesses (Figure 1). This is seen in the common usage of continuous processes for ultrasonic welding of plastic fabrics or films [16] and even for automated placement of thermoplastic composite prepreg tows. In the case of stiff composite plates or parts, however, the cold energy director ahead of the sonotrode (with a typical thickness of around 0.25 mm for flat EDs [6] and 0.5 mm for triangular EDs [11]) is expected to stop or slow down the squeeze flow and therefore, have an undesirable effect on the welding process and weld quality.

The authors' approach to solve this issue is to develop a zero-flow continuous ultrasonic welding process, i.e. a process with zero vertical displacement of the sonotrode. Previous research on thin EDs [17] for the welding of carbon fiber reinforced polyetherimide (CF/PEI) composites showed that when the flat ED became very thin (in the order of hundredths of a millimeter), the static welding process could be successfully completed with no to very little squeeze flow at the welding interface. Consequently, the present paper aims at experimentally validating zero-flow on continuous ultrasonic welding of carbon fiber reinforced polyphenylene sulfide

(CF/PPS) composites based on the use of thin EDs by: (i) determining the ED thickness that allows welding with no to very little squeeze-flow at the welding interface, (ii) assessing applicability of zero-flow welding to spot welds where the downward displacement of the sonotrode is constrained by cold ED, and (iii) assessing the applicability of zero-flow welding to continuous ultrasonic welding.

Experimental

Materials and samples manufacturing

The composite material used in this study was carbon fiber (5 harness satin fabric) reinforced CF/PPS from Ten Cate Advanced Composites, The Netherlands (CETEX®). Laminates with a $[0/90]_{3S}$ ply architecture and 1.92 mm nominal thickness were manufactured from powder-impregnated prepreg. Consolidation was performed in a hot platen press at 320°C and 1 MPa for 20 min, following the recommendations of the manufacturer. Flat energy directors with different thicknesses were manufactured by stacking several layers of 0.08 mm-thick neat PPS film (Fortron® PPS, Celanese, USA) in a hot platen press at 260°C and 2 MPa for 10 min. Three ED thicknesses were considered in the first part of this study: 0.08 mm (EDs directly cut from the original PPS film), 0.16 mm (hot-stacking of two PPS film layers) and 0.24 mm (hot-stacking of three PPS film layers). Note that the temperature at which the EDs were manufactured was below the melting temperature of PPS. The reason for this was to achieve good control of the ED thickness by preventing polymer flow.

Three different types of single-lap welded samples were considered in this study: (i) regular samples with a fully welded overlap, shown in Figure 2; (ii) spot-welded samples with an overlap approximately twice as big as the total welded area, as indicated in Figure 3; and (iii) continuous-welded samples with a fully welded overlap,

as shown in Figure 4. The adherends used to create these different types of welded samples were cut with a water-cooled circular diamond saw from the CF/PPS laminates to the dimensions indicated in Figures 2 to 4. Prior to welding, adherends and ED were degreased and the ED, which covered the complete overlap for all three types of samples, was secured to the bottom adherend by using adhesive tape.

Ultrasonic welding processes

Regular and spot-welded samples (Figures 2 and 3, respectively) were welded using the off-the-shelf microprocessor-controlled Dynamic 3000 ultrasonic welder (Rinco Ultrasonics, Switzerland), as shown in Figure 5. This static ultrasonic welder operated at 20kHz and delivered constant vibration amplitude and a maximum power of 3000 W. In order to keep the adherends in place throughout the welding process and, when applicable, to allow for vertical displacement of the top adherend during squeeze-flow of the ED, a custom-designed clamping fixture, as shown in Figure 5, was used. For the regular welds (Figure 2) a 40 mm-diameter cylindrical titanium sonotrode (Figure 5) was used. For the spot welds (Figure 3), a rectangular sonotrode with a 14.9 mm x 30 mm contact area was employed. In both cases, the welding force was 1000 N, corresponding to a weld pressure of 3.1 MPa for the regular welds (12.7 mm x 25.4 mm contact area between sonotrode and welding stack, Figure 2) and 2.6 MPa for the spot welds (14.9 mm x 25.4 mm contact area between sonotrode and welding stack, Figure 3). The peak-to-peak vibration amplitude was around 85 μm (86.2 μm for the cylindrical sonotrode and 84.6 μm for the rectangular sonotrode, owing to different gain factors). After the vibration phase, 1000 N force continued to be applied for four seconds to consolidate the weld during cooling. Either the displacement of the sonotrode or the welding energy was used to indirectly control the duration of the vibration phase of the welding process.

The continuous-welded samples (Figure 4) were produced using the basic custom-built continuous ultrasonic welder shown in Figure 6. This welder featured an ultrasonic welding train (converter, booster and sonotrode) and a pneumatic press, both of them mounted on a horizontal moving platform. A stepper motor was used to translate the platform along a fixed axis. Therefore, in the continuous welding process used in this study, the adherends remained stationary whilst the sonotrode moved along the weld line. More specifically, the process was designed so that the sonotrode would lower, get into contact with the top adherend, build up the welding force in one second and subsequently, start vibrating and moving at a given constant speed until a prescribed welding distance was reached. The weld length was defined as the center-to-center distance of the sonotrode when located at both edges of the weld line, as indicated in Figure 4. The clamping system consisted of two aluminium bars, one on top of each adherend, bolted to a base plate with a torque of 20 Nm.

The converter (C20-10, Rinco Ultrasonics, Switzerland) of the continuous ultrasonic welder operated at 20 kHz and delivered constant vibration amplitude and a maximum continuous power of 1200 W. The rectangular sonotrode with a 14.9 mm x 30 mm contact area used to obtain the static spot welds, was also used in the continuous ultrasonic welding setup. A welding force of 500 N was selected in order to deliver 2.6 MPa welding pressure (12.7 mm x 14.9 mm between sonotrode and welding stack, see Figure 4). It should be noted that due to the expected impact of the welding pressure on the squeeze flow of the energy director [6], an effort was made to keep the welding pressures as similar as possible in the three welding processes considered in this research. Based on preliminary experiments and owing to the lower power delivered by the converter used in the continuous ultrasonic welder, as compared to the static ultrasonic welder, the peak-to-peak vibration amplitude was reduced to 49.5 μm . For

this first proof of concept, no compaction device was utilised to consolidate the weld upon cooling. The duration of the welding process was controlled through the translational speed of the sonotrode.

Methodology, testing and analysis

The regular welds (Figure 2) were used to determine the ED thickness that would allow high-quality welding with little to no squeeze flow of the ED, i.e., little to no downward displacement of the sonotrode. Subsequently, the spot welds (Figure 3) were used to assess zero-flow welding with downward displacement of the sonotrode constrained by the cold ED. Finally, continuous welding (Figure 4) was performed to evaluate the viability of the zero-flow approach. The feedback data provided by the ultrasonic welder on the dissipated power and the vertical displacement of the sonotrode during the vibration phase of the process were used to investigate the effect of changes in ED thickness and welding configuration. Single-lap shear testing based on the ASTM D 1002 standard was performed to quantify the strength and hence the quality of the welded joints. For the regular and spot welds, the as-welded samples were directly used for mechanical testing. In the case of continuous welds, the welded samples were cut in five individual coupons (approximately 20 mm wide). The apparent lap shear strength (LSS) of the welded joints was calculated as the maximum load during the test divided by the overlap area (regular and continuous welds) or by the area covered by the sonotrode (spot welds). Naked-eye or microscopy (Keyence VHX-2000E digital microscope) observation of the fracture surfaces after mechanical testing was also used to assess the quality of the welded joints.

It should be noted that the temperature at the welding interface was not measured in any of the welding processes used in this work. This is due to experimental difficulties resulting from either lack of access for infrared thermography measurements

at the welding area or thermocouples affecting the heat generation process when placed at the interface. However, the analysis of the feedback data provided by the ultrasonic welder, together with the output of the mechanical tests and fractography analysis of welded joints, were found to provide enough information to assess the viability of continuous ultrasonic welding of CF/PPS composite plates using the zero-flow approach.

Results and discussion

ED thickness for zero-flow ultrasonic welding

Representative power and displacement curves for the regular welds obtained with 0.16 mm and 0.24 mm-thick EDs are shown in Figure 7. Power and displacement curves obtained with 0.08 mm-thick EDs are presented in Figure 8. Typical characteristics, common to welding processes that rely on the occurrence of downward displacement of the sonotrode, i.e. squeeze flow of the ED, are found in the curves of both the 0.16 mm and 0.24 mm-thick EDs (Figure 7). These characteristics are a first power peak during the phase in which the sonotrode remains nearly stationary and a second power peak/plateau in the phase during which downward displacement of the sonotrode occurs. The first peak is associated with the first occurrence of local melting in the ED. The second peak/plateau corresponds to two simultaneous events: squeeze flow of the molten ED and melting of the resin in the first layer of each composite adherend [6]. The latter enables autohesion and thus, the creation of a proper weld between the two adherends [7].

In the case of the 0.08 mm-thick ED, the power curves remain relatively flat after an initial steep increase, showing a small peak right after the onset of downward sonotrode displacement (Figure 8). These relatively flat power curves are consistent

with the observations for CF/PEI samples welded with thin EDs [17] and are associated with simultaneous melting of the ED and of the first layer of each adherend near the onset of the downward displacement of the sonotrode. Owing to the early melting of the first layers of the adherends, i.e. before any significant downward displacement takes place, 0.08 mm-thick EDs show potential to provide high-strength welds after little or no squeeze flow at the welding interface. This potential is further confirmed by the results of mechanical tests on samples welded at different stages in the welding process. Figure 9 shows the lap shear strength yielded by these samples with respect to the displacement at the end of the vibration phase as determined from the curves provided by the welder. It must be noted that both displacement-controlled welding and energy-controlled welding were used to obtain the wide range of displacement values shown in Figure 9. The LSS versus displacement plot was however considered as the most relevant in order to ascertain whether the 0.08 mm-thick ED would provide sufficient weld strength at little to no downward displacement of the sonotrode. The LSS versus displacement plot indicates that maximum strength is indeed obtained between 0 and 0.01 mm, which approximately coincides with the peaks in the power curves shown in Figure 8.

As explained before, zero-squeeze flow is considered as the target for continuous ultrasonic welding in this work, which corresponds to 0 mm displacement in Figure 9. For that case, the maximum achievable LSS is equal to 31.9 ± 0.9 MPa (based on 5 samples) which is around 12% lower than the LSS yielded by welds with a 0.24 mm-thick ED (namely, 36.5 ± 0.9 MPa, obtained with 3 samples). The latter were welded using a traditional displacement-controlled welding process with 0.15 mm displacement, determined from the second peak in the power curves in Figure 7 [7]. Fracture surface analysis, shown in Figure 10, indicates that this 12% drop in LSS could

be caused by un-welded areas, consistently observed in the samples welded with 0.08 mm-thick ED and which are believed to result from a non-uniform temperature distribution at the welding interface. This non-uniform temperature distribution could be attributed to different factors, among which are uneven contact between the sonotrode and the top adherends or uneven distribution of the amplitude of vibration at the base of the sonotrode. Moreover, it is assumed to be aggravated by the virtual absence of flow at the interface during welding. Squeeze flow of the molten ED can be expected to even out a potential non-uniform temperature distribution at the welding interface through forced convection from the molten polymer. However, the observed drop in LSS is relatively small and the movement of the sonotrode in the continuous ultrasonic welding process is expected to help improve temperature uniformity caused by local changes in amplitude or in contact pressure. Additionally, it must be noted that, unlike the results reported in [17] for the welding of CF/PEI composites, no signs of overheating in the form of evident porosity could be observed on the fracture surfaces of CF/PPS samples welded with 0.08 mm-thick EDs (see detail in Figure 10).

Zero-flow spot welding

Representative power and displacement curves for spot welds with a 0.08 mm-thick ED are shown in Figure 11. The term “spot weld” refers to a welded joint in which the welded area is smaller than the total overlap (Figure 3). Spot welds are considered as an intermediate step towards continuous ultrasonic welding, since in both cases, the cold ED around the weld zone restricts the downward displacement of the sonotrode. The curves in Figure 11 for spot welds share a similar trend to regular welds with 0.08 mm-thick EDs, as seen in Figure 8. In particular, flattening of the power curves after the initial rapid increase is observed in both cases. An interesting difference between the curves in Figures 8 and 11 is that the maximum upward displacement reached by the

sonotrode (negative displacement in Figures 8 and 11) is significantly higher in the case of the spot welds (-0.05 mm versus -0.01 mm). This negative displacement at the beginning of the welding process is believed to be affected by a combination of two counteracting effects. One of them is the thermal expansion of the energy director as it heats up, which causes upward displacement of the sonotrode (negative displacement). The other one is the softening of the energy director when its temperature increases, which, in the absence of constraints, will allow the sonotrode to compress it (positive displacement). In the case of the spot welds, the extra ED on both sides of the welding area can be assumed to not heat up as much as the ED right under the sonotrode. Consequently, this extra ED prevents any further compression of the welding interface resulting in thermal expansion playing a dominant role in the displacement of the sonotrode.

The feasibility of zero-flow spot welding with a 0.08 mm-thick ED was assessed through testing of spot welds in optimum welding conditions and by comparing them to those obtained with a traditional 0.24 mm-thick ED. In order to define optimum welding conditions, samples were spot welded at three energy levels, namely 300, 400 and 500 J, all of them within the flat-power region in Figure 11. Due to the negative displacement of the sonotrode in this region, the welding process could no longer be displacement-controlled and hence, energy was used as the controlling parameter. The optimum welding energy was chosen to be 400 J since it provided no visible signs of overheating and the fewest un-welded areas (Figure 12). The LSS yielded by five samples welded at 400 J is 30.7 ± 4.3 MPa. This value is comparable to the LSS of the regular welds with a 0.08 mm-thick ED (namely 31.9 ± 0.9 MPa). The higher scatter in the case of the spot welds is attributed to the fact that the welded area did not exactly

coincide with the area of the sonotrode. This, however, should not pose a problem in the continuous welding process owing to the movement of the sonotrode.

Finally, spot welds with a 0.24 mm-thick ED exhibit low quality welds with a highly non-uniform appearance as shown in Figure 13, also observed in our previous work [14]. This result further confirms the appropriateness of the 0.08 mm-thick ED for the zero-flow spot welds considered in this study and, consequently, for zero-flow continuous ultrasonic welding as the natural step forward.

Zero-flow continuous welding

In the basic continuous ultrasonic welding setup used in this study, the main controlling parameter is the translational speed of the sonotrode, referred to as ‘welding speed’.

Based on the average vibration times obtained for the regular and spot welds (between 250 and 300 ms, approximately), four welding speeds were proposed for the zero-flow continuous welding process: 40, 60, 80 and 100 mm/s. Welding at 40 mm/s resulted in severe overheating on the surface of the adherend in contact with the sonotrode and hence, it was not investigated further. Welding speeds equal to and above 60 mm/s caused little to no damage on the adherends.

The LSS values yielded by each of the five coupons, cut from the 100 mm-long continuously welded panels, for 60, 80 and 100 mm/s welding speeds, are shown in Figure 14. The LSS values obtained at 60 mm/s are overall higher than those obtained at 80 and 100 mm/s. The analysis of the corresponding fracture surfaces in Figure 15 reveals numerous un-welded areas at 80 and 100 mm/s, which explains their low LSS. A 60 mm/s welding speed, on the other hand, results in a much more effective welding process. However, un-welded areas can still be observed at both ends of the weld line (samples 1 and 5, respectively). This is understandable considering that at the beginning and end of the weld, the adherends do not face the complete width of the sonotrode, i.e.

the effective weld times are lower. Improving the quality at the edges would probably require modifying the starting and ending position of the sonotrode or slowing down its movement both at the beginning and end of the weld line.

Disregarding the contribution of the edge coupons, the average LSS at 60 mm/s welding speed is equal to 29.5 ± 4.9 MPa, which is, even for this basic continuous ultrasonic welding process, already comparable to the LSS yielded by the zero-flow spot welds and regular welds (30.7 ± 4.3 MPa and 31.9 ± 0.9 MPa, respectively). A closer look at the fracture surfaces of the continuous welds indicates insufficient consolidation pressure through the presence of numerous voids, which are commonly found on fracture surfaces of welds where the force is released right after the vibration phase (Figure 16). Consequently, adding a consolidation device to the continuous ultrasonic welder could be expected to further increase the strength of the zero-flow continuous welds.

Conclusions

This paper presented a novel zero-flow continuous ultrasonic welding process for CF/PPS thermoplastic composites. Zero-flow welding, i.e. a welding procedure in which no squeeze flow of the energy director is required to achieve sufficient weld strength, is enabled by the use of very thin (0.08 mm) flat energy directors. The zero-flow approach allows continuous welding of stiff thermoplastic composite plates since it does not require local deformation of the adherends as the sonotrode moves along the weld line. The results presented in this paper for a basic zero-flow continuous ultrasonic welding process prove its feasibility and indicate its potential to deliver high-strength welded seams at very high speed. Consequently, zero-flow continuous ultrasonic welding is expected to play a significant role in structural joining of thermoplastic composite assemblies of the future.

Acknowledgments

The authors would like to thank Rudolf Dasbach (AESON B.V., The Netherlands) for his help on the design of the continuous ultrasonic welding setup used in this research.

References

1. I.F. Villegas, L. Moser, A. Yousefpour, P. Mitschang and H.E.N. Bersee: 'Process and performance evaluation of ultrasonic, induction and resistance welding of advanced thermoplastic composites', *J. Thermoplastic Compos.*, 2012, **26**, (8), 1007-1024.
2. A. Levy, S. Le Corre and I.F. Villegas: 'Modelling of the heating phenomena in ultrasonic welding of thermoplastic composites with flat energy directors', *J. Mater. Process. Tech.*, 2014, **214**, 1361-1371.
3. H. Potente: 'Ultrasonic welding – Principles and theory', *Materials and Design*, 1984, **5**(5), 228-234.
4. I.F. Villegas, B. Valle Grande, H.E.N. Bersee and R. Benedictus R: 'A comparative evaluation between flat and traditional energy directors for ultrasonic welding of CF/PPS composites', *Compos. Interface*, 2015, **22**(8), 717-729.
5. A. Benatar and T.G. Gutowski: 'Ultrasonic welding of PEEK graphite APC2 composites', *Polym. Eng. Sci.*, 1989, **29**(23), 1705-1721.
6. I.F. Villegas: 'In-situ monitoring of ultrasonic welding of thermoplastic composites through power and displacement data', *J. Thermoplastic Compos.*, 2015, **28**(1), 66-85.
7. I.F. Villegas: 'Strength development versus process data in ultrasonic welding of thermoplastic composites with flat energy directors and its application to the definition of optimum processing parameters', *Compos. Part A-Appl. S.*, 2014, **65**, 27-37.
8. J.W. Van Ingen, A. Buitenhuis, M. van Wijngaarden and F. Simmons III: 'Development of the Gulfstream G650 induction welded thermoplastic elevators and rudder', Proc. Int. SAMPE Symposium and Exhibition, Seattle, USA, May 2010.

9. S. Becker, D. Maurer, M. Duhdovic and P. Mitschang: 'Quality-controlled continuous induction welding of CFRP composites', *JEC Composites Magazine*, 2015, **52**(101), 40-43.
10. S. Pappadà, A. Salomi, J. Montanaro, A. Passaro, A. Caruso and A. Maffezzoli, 'Fabrication of a thermoplastic matrix composite panel by induction welding', *Aerosp. Sci. Technol.*, 2015, **43**, 314-320.
11. H.M. Lu, A. Benatar and F.G. He: 'Sequential ultrasonic welding of PEEK/graphite composite plates', Proc. ANTEC Conf., Montreal, Canada, May 1991, **37**, 2523-2526.
12. E. Soccard: 'Ultrasonic assembly method', Patent no: WO 2007/003626 A1, EADS CCR, 2007.
13. A. Levy, S. Le Corre and A. Poitou: 'Ultrasonic welding of thermoplastic composites: a numerical analysis at the mesoscopic scale relating processing parameters of polymer and quality of adhesion', *International Journal of Material Forming*, 2014, **7**(1), 39-51.
14. G. Palardy, F.M. Agricola, C. Dransfeld and I.F. Villegas: 'Up-scaling of the ultrasonic welding process for joining thermoplastic composites', Proc. SAMPE Conf., Baltimore, USA, May 2015.
15. I.F. Villegas and G. Palardy: 'Ultrasonic welding of CF/PPS composites with integrated triangular energy directors: melting, flow and weld strength development', *Compos. Interface*, 2016, DOI:10.1080/09276440.2017.1236626.
16. E. Lokensgard: 'Industrial Plastics: Theory and Applications', 5th edn, 2010, Delmar, Cengage Learning.
17. G. Palardy and I.F. Villegas: 'On the effect of flat energy director thickness on heat generation during ultrasonic welding of thermoplastic composites', *Compos. Interface*, 2017, **24**(2), 203-214, DOI:10.1080/09276440.2016.1199149.

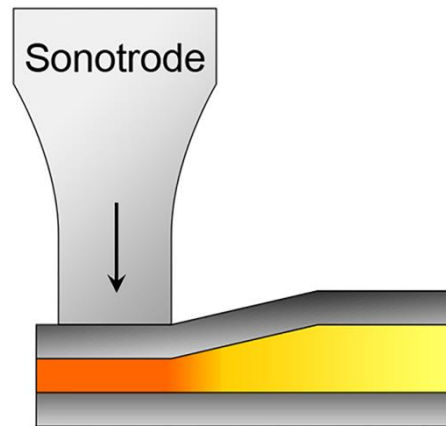


Figure 1. Effect of squeeze flow of molten energy director in continuous ultrasonic welding. The arrow indicates the direction of welding force and vibration amplitude.

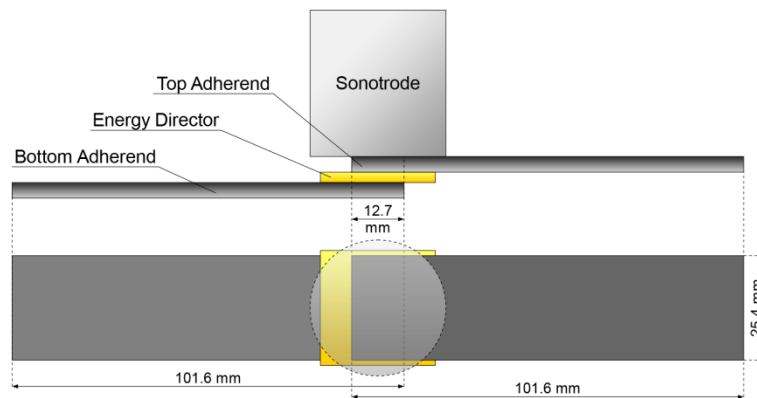


Figure 2. Schematic of the regular welded sample used in this study (dimensions are not to scale).

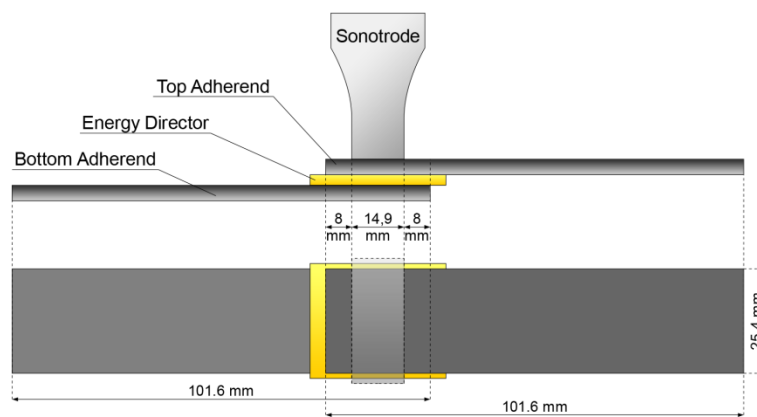


Figure 3. Schematic of the spot welded sample used in this study (dimensions are not to scale).

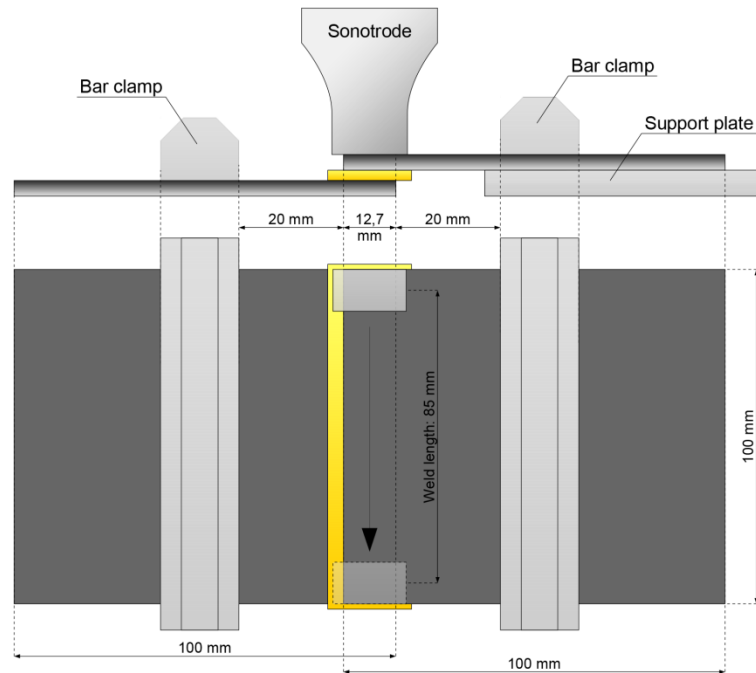


Figure 4. Schematic of the continuous welded sample used in this study (dimensions are not to scale).

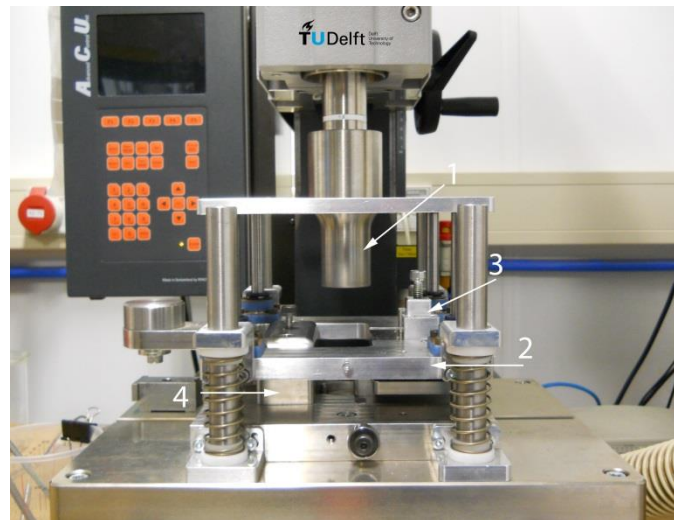


Figure 5. Ultrasonic welder with cylindrical sonotrode and custom-designed welding fixture for regular and spot welds (1: cylindrical sonotrode, 2: sliding platform for top clamp, 3: top clamp, 4: bottom clamp).

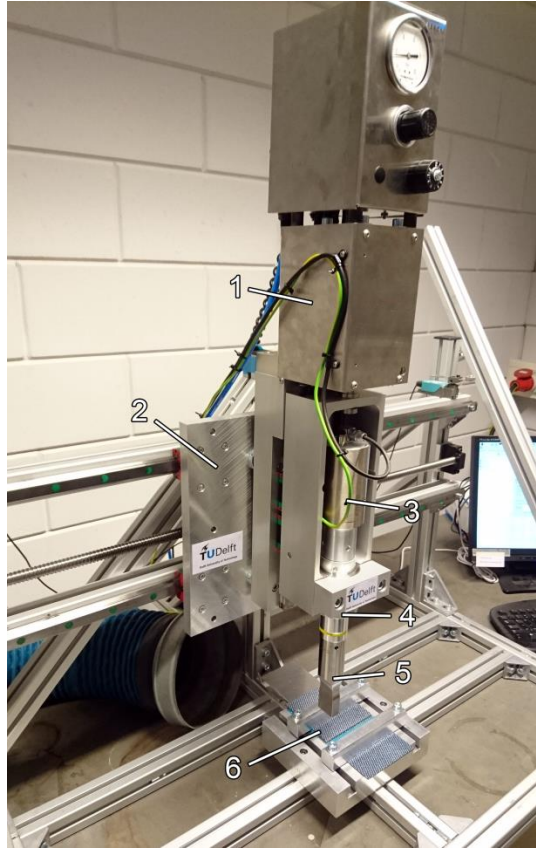


Figure 6. Setup for continuous ultrasonic welding (1: pneumatic press, 2: horizontal moving platform, 3: converter, 4: booster, 5: sonotrode, 6: clamped adherends).

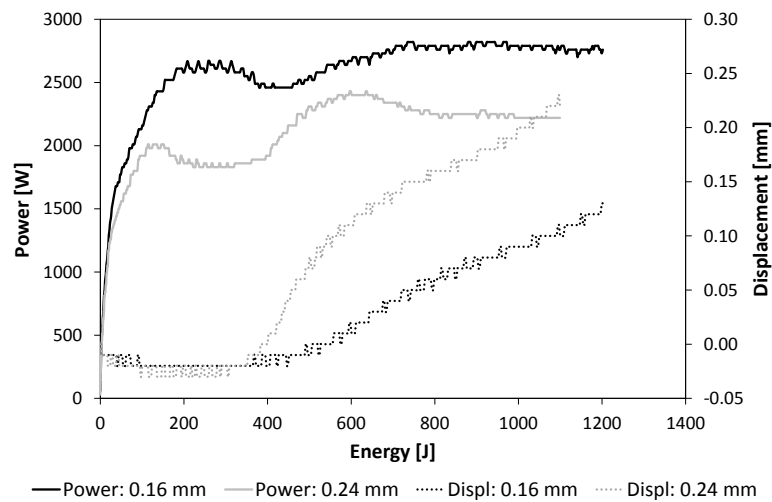


Figure 7. Representative power and displacement curves for 0.16 mm and 0.24 mm-thick EDs (1000 N welding force, 86.2 μ m vibration amplitude, displacement-

controlled welding). A positive displacement value corresponds to downward movement of the sonotrode.

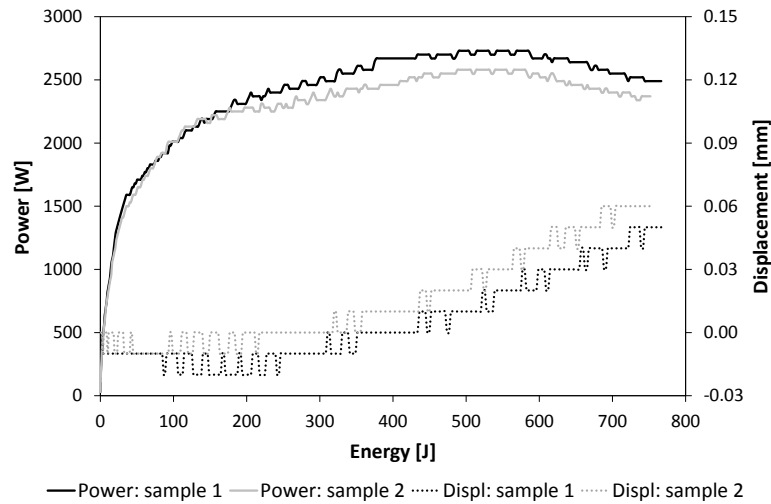


Figure 8. Representative power and displacement curves for two samples welded with 0.08 mm-thick EDs (1000 N welding force, 86.2 μm vibration amplitude, displacement-controlled welding). A positive displacement value corresponds to downward movement of the sonotrode.

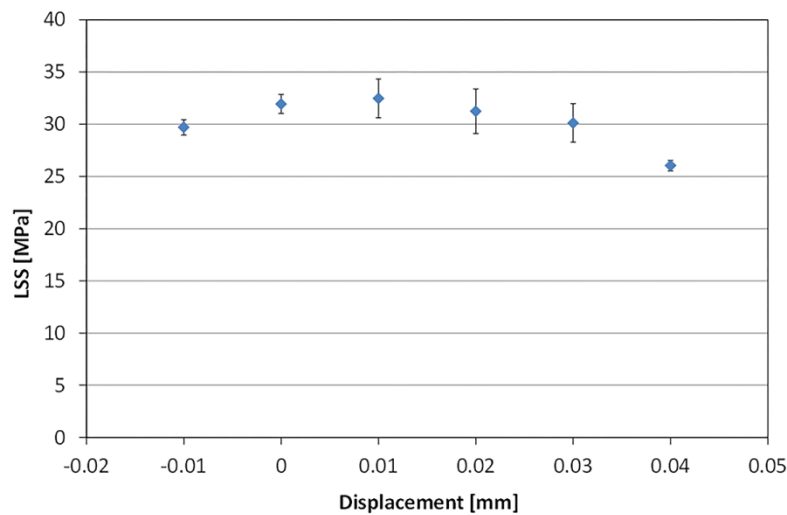


Figure 9. Lap shear strength versus displacement for 0.08 mm-thick ED. Samples were welded at different stages in the welding process. Both energy-controlled (energy values ranging from 400 to 800 J) and displacement-controlled (0.01 and 0.02 mm input displacement) welding processes were used to obtain the data points in this plot.

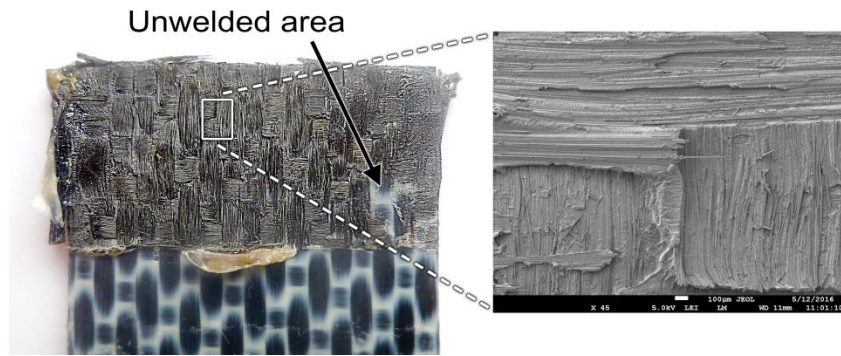


Figure 10. Fracture surface and SEM detail for sample welded with 0.08 mm-thick ED (1000 N welding force, 86.2 μm vibration amplitude, 0.01 mm displacement).

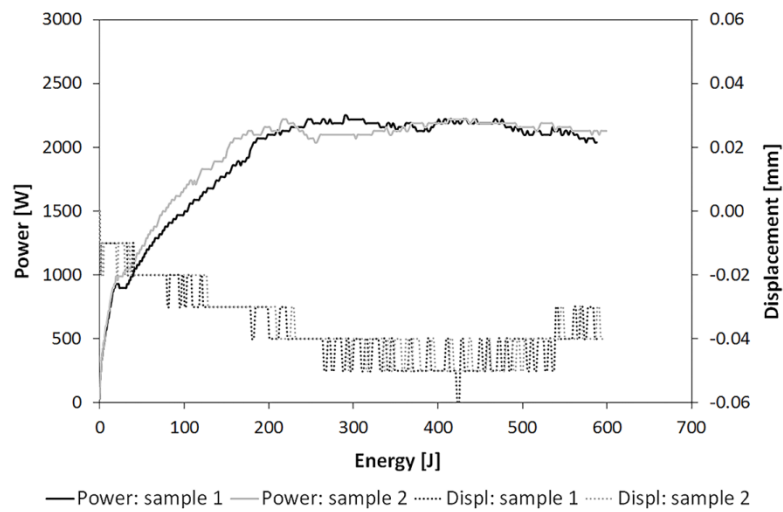
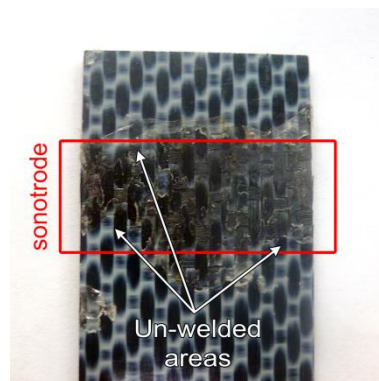
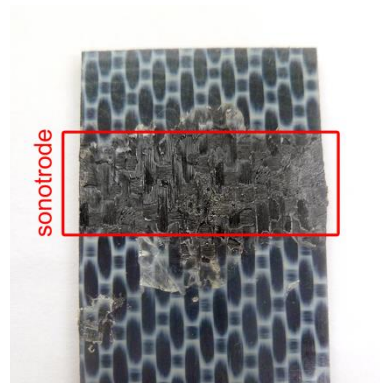


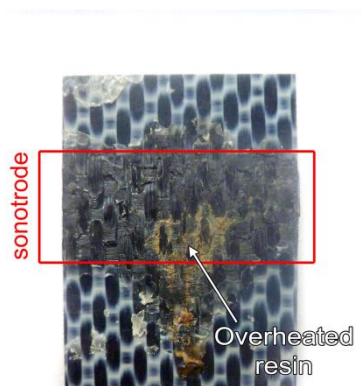
Figure 11. Representative power and displacement curves for two spot-welded samples with 0.08 mm-thick ED (1000 N welding force, 84.6 μm vibration amplitude). A positive displacement value corresponds to downward movement of the sonotrode.



(a)



(b)



(c)

Figure 12. Representative fracture surfaces from spot welds obtained at different welding energies: (a) 300 J, (b) 400 J and (c) 500 J.

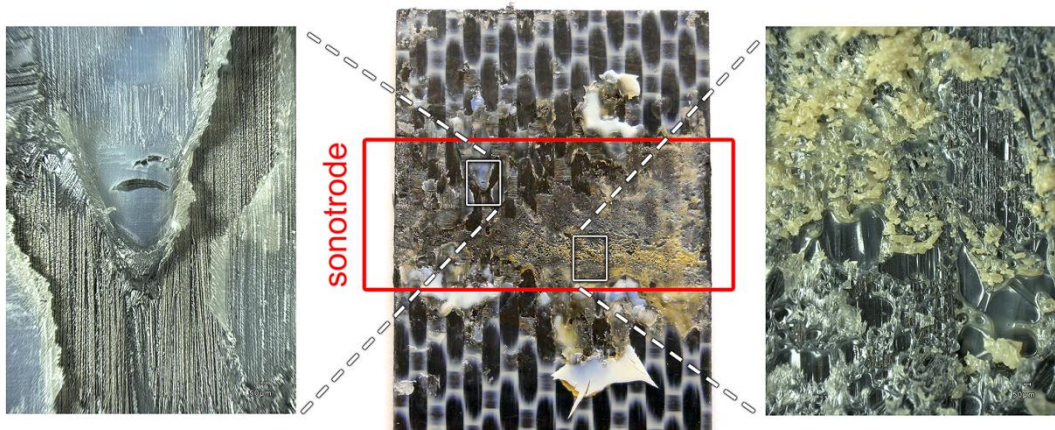


Figure 13. Fracture surface of a spot weld obtained with a 0.24 mm-thick ED and 600 J welding energy.

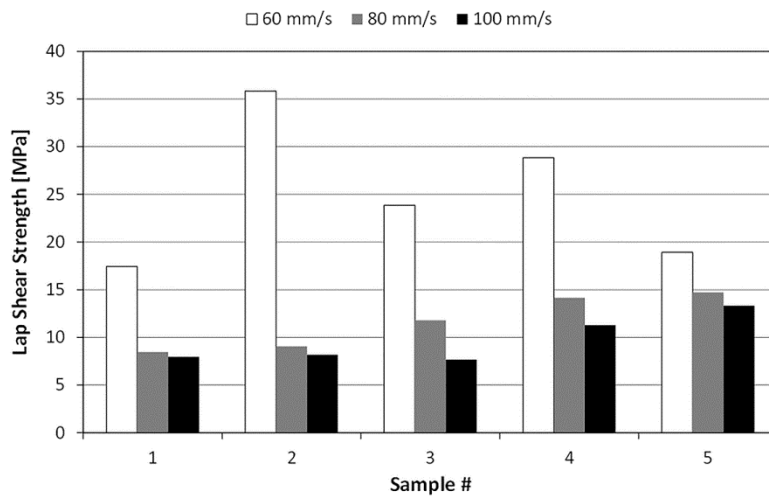


Figure 14. LSS of individual coupons cut from continuously welded panel at three different welding speeds: 60, 80 and 100 mm/s.

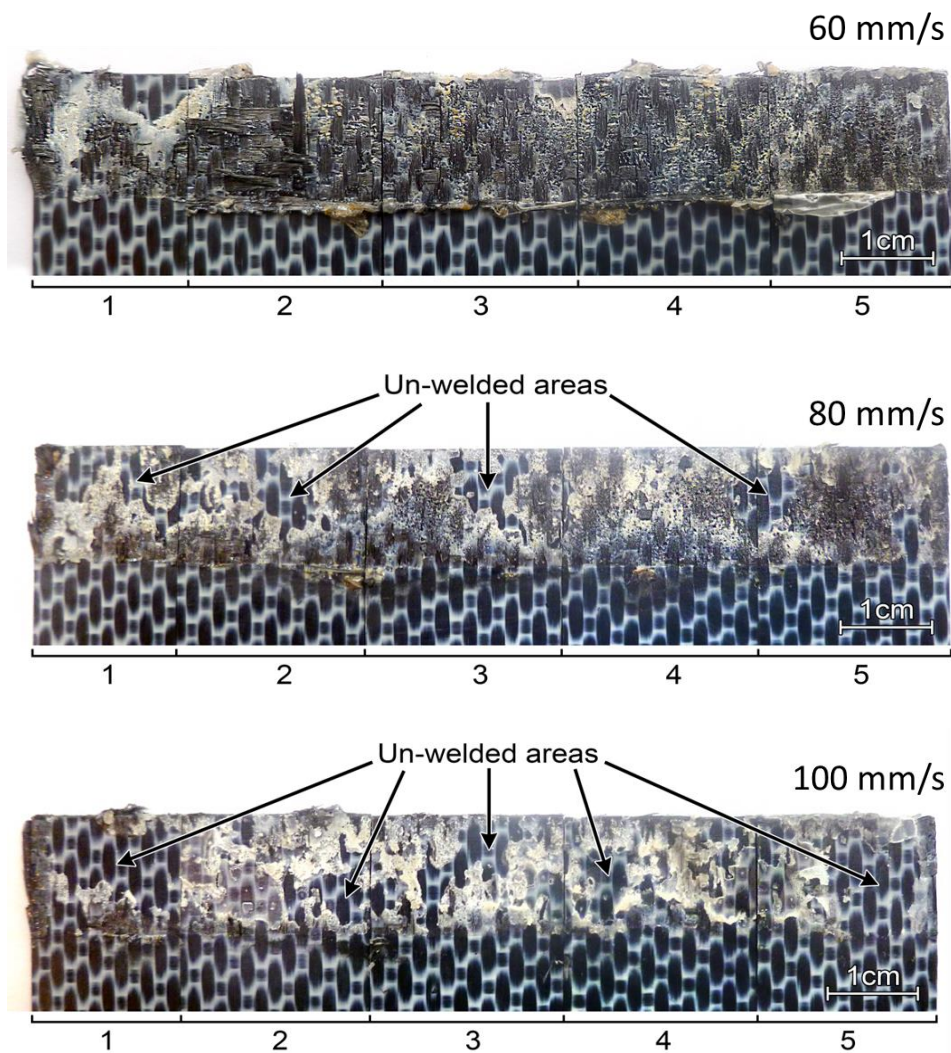


Figure 15. Fracture surfaces of samples welded at 60, 80 and 100 mm/s (from top to bottom).



(a)



(b)

Figure 16. (a) Detail from fracture surface on sample welded at 60 mm/s showing similar porosity to that found in samples on which force was released right after vibration, (b) Detail from fracture surface on regular sample on which force was released right after vibration. Scale bars: 50 μm.

Figure 1. Effect of squeeze flow of molten energy director in continuous ultrasonic welding. The arrow indicates the direction of welding force and vibration amplitude.

Figure 2. Schematic of the regular welded sample used in this study (dimensions are not to scale).

Figure 3. Schematic of the spot welded sample used in this study (dimensions are not to scale).

Figure 4. Schematic of the continuous welded sample used in this study (dimensions are not to scale).

Figure 5. Ultrasonic welder with cylindrical sonotrode and custom-designed welding fixture for regular and spot welds (1: cylindrical sonotrode, 2: sliding platform for top clamp, 3: top clamp, 4: bottom clamp).

Figure 6. Setup for continuous ultrasonic welding (1: pneumatic press, 2: horizontal moving platform, 3: converter, 4: booster, 5: sonotrode, 6: clamped adherends).

Figure 7. Representative power and displacement curves for 0.24 mm and 0.16 mm-thick EDs (1000 N welding force, 86.2 μm vibration amplitude, displacement-controlled welding). A positive displacement value corresponds to downward movement of the sonotrode.

Figure 8. Representative power and displacement curves for two samples welded with 0.08 mm-thick EDs (1000 N welding force, 86.2 μm vibration amplitude, displacement-controlled welding). A positive displacement value corresponds to downward movement of the sonotrode.

Figure 9. Lap shear strength versus displacement for 0.08 mm-thick ED. Samples were welded at different stage in the welding process. Both energy-controlled (energy values ranging from 400 to 800 J) and displacement-controlled (0.01 and 0.02 mm input displacement) welding processes were used to obtain the data points in this plot.

Figure 10. Fracture surface and SEM detail for sample welded with 0.08 mm-thick ED (1000 N welding force, 86.2 μm vibration amplitude, 0.01 mm displacement).

Figure 11. Representative power and displacement curves for two spot-welded samples with 0.08 mm-thick ED (1000 N welding force, 84.6 μm vibration amplitude). A positive displacement value corresponds to downward movement of the sonotrode.

Figure 12. Representative fracture surfaces from spot welds obtained at different welding energies: (a) 300 J, (b) 400 J and (c) 500 J.

Figure 13. Fracture surface of a spot weld obtained with a 0.24 mm-thick ED and 600 J welding energy.

Figure 14. LSS of individual coupons cut from continuously welded panel at three different welding speeds: 60, 80 and 100 mm/s.

Figure 15. Fracture surfaces of samples welded at 60, 80 and 100 mm/s (from top to bottom).

Figure 16. (a) Detail from fracture surface on sample welded at 60 mm/s showing similar porosity to that found in samples on which force was released right after vibration, (b) Detail from fracture surface on regular sample on which force was released right after vibration. Scale bars: 50 μm .